Available online at www.sciencedirect.com
ScienceDirect
European Journal of Mechanics B/Fluids 26 (2007) 284–294

Numerical analysis of the nonlinear vibration of axisymmetric liquid bridges

J.M. Montanero

Departamento de Electrónica e Ingeniería Electromecánica, Universidad de Extremadura, E-06071 Badajoz, Spain

Received 9 January 2006; received in revised form 26 April 2006; accepted 9 June 2006

Available online 20 July 2006

Abstract

The vibration of axisymmetric liquid bridges is analyzed numerically in the framework of the one-dimensional approximation. Nonlinear effects on both the interface deformation and velocity field are studied. The solutions of the Lee, average, and Cosserat models are compared. For the Cosserat model, the results are compared with those obtained from an asymptotic analysis performed in the Plateau–Rayleigh stability limit. In addition, some results concerning the influence of the viscosity on the linear vibrations are reported.

PACS: 68.35.J; 68.10.C; 47.11.+j

Keywords: Liquid bridge; Nonlinear dynamics; One-dimensional models; Vibrations

1. Introduction

The vibration of liquid bridges in the linear regime has frequently been studied over the past years both theoretically and experimentally. The theoretical studies have mainly been focused on the calculation of the resonance frequencies from the three-dimensional (3D) Navier–Stokes equations for inviscid [1] and viscous [2] cylindrical liquid bridges. Because of the complex dependence of the surface tension force on the interface deformation, one-dimensional (1D) models have been proposed to analyze the behaviour of axisymmetric shapes [4–8]. In this context, the Lee,[1] averaged, and parabolic models are derived by substituting a truncated Taylor series in the radial coordinate of the hydrodynamic fields into the Navier–Stokes equations and boundary conditions at the interface. Also, the Cosserat model is derived by introducing the mean axial velocity into the parabolic model [7–9]. Basically, one assumes that the radial momentum flux is small compared with the axial momentum flux, which uncouples the radial and axial momentum equations. It is known that all these models generally describe with accuracy the linear dynamic response of a moderately slender liquid bridge for frequencies of the order of its first natural frequency [10–13]. Noticeable exceptions are the recirculating velocity patterns associated with the hydrodynamic modes [10], which cannot be de-

E-mail address: jmm@unex.es (J.M. Montanero).

[1] The original derivation of the Lee model did not include the effect of viscosity. A systematic derivation of this model including that effect can be found in [3].

0997-7546/$ – see front matter
doi:10.1016/j.euromechflu.2006.06.002

scribed from these models. On the experimental side, the linear vibration of a liquid bridge has been considered in several works [9,14–17]. The resonance frequencies measured using the Plateau–Rayleigh technique [9,14,17] and microzones [15,16] were in good agreement with those predicted by both 3D and 1D approaches.

Most of the studies dealing with nonlinear dynamics of liquid bridges have focused on the dynamic stability and the breakup process (see, e.g., [4–6,18–22] and references therein), where the 1D approximation provides results in qualitative agreement with experimental observations. The nonlinear vibration of liquid bridges has been considered in only a few works. The 3D Navier–Stokes equations were numerically integrated to calculate the evolution of an axisymmetric liquid bridge and to obtain its resonance frequencies in the nonlinear regime [23]. The theoretical predictions were in good agreement with the experiments [24]. The 3D description has also been considered to analyze the steady streaming flow due to vibration of cylindrical liquid bridges in some limiting cases [25,26]. Within the context of the 1D theory, a self-similar solution to the Cosserat model was obtained with the singular perturbation method to describe the nonlinear behaviour of liquid bridges asymptotically close to the Plateau–Rayleigh stability limit [18]. This solution has been used to describe the breakup process [18], the dynamical stability [19], and the vibration [27,28] of axisymmetric liquid bridges.

The main goal of the present study is to describe the nonlinear vibration of axisymmetric viscous liquid bridges within the framework of the 1D approximation. To this end, the Lee, average, and Cosserat models are integrated by means of a fully implicit finite difference scheme. Nonlinear effects are clearly appreciated for moderately large interface deformations. The results provided by the three models are compared, showing excellent agreement even when nonlinear effects are present. A comparison with the self-similar solution obtained by Rivas and Meseguer [18] is carried out for configurations close to the Plateau–Rayleigh stability limit. Good agreement is observed for the interface deformation, while significant discrepancies are found for the velocity field. In addition, and in order to complete a previous study for inviscid liquid bridges [11], the influence of the viscosity on small-amplitude vibrations is analyzed. Some results related to this analysis were obtained in Ref. [9] from a different numerical technique.

2. Formulation of the problem

The fluid configuration considered is sketched in Fig. 1. It consists of an isothermal mass of liquid of volume $\widetilde{V}$, held between two parallel coaxial disks placed a distance L apart. The radii of the disks are $r_0(1-H)$ and $r_0(1+H)$. Due to the sharpness of the disk edges, one assumes that the liquid anchors perfectly to those edges, preventing motion of the triple contact line. The liquid bridge is subjected to the action of an axial constant force (gravity) of magnitude g_0 per unit mass. The liquid bridge density is ρ, the viscosity is μ, and the surface tension associated with the interface is σ. These properties are uniform and constant under the present conditions of isothermal analysis. The surrounding gas has negligible density and viscosity, so that it does not affect the dynamics of the liquid bridge. For this axisymmetric configuration the equilibrium contour of the liquid bridge is characterized by the function $F_0(z)$, which measures the distance between a surface element and the axis z of the disks.

Let us now consider the vibration along the z axis of the above fluid configuration together with the supporting disks. The vibration starts at the instant $t = 0$, and is harmonic of amplitude A and angular speed ω. The axial

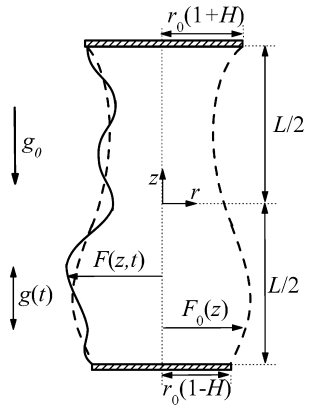

Fig. 1. Geometry and coordinate system for the liquid bridge.

component of the inertial force per unit mass produced by the vibration is $g(t) = -A\omega^2 \sin(\omega t)$ for $t \geqslant 0$. The function $F(z,t)$ measures the distance between a surface element and the z axis at the instant t, while $W(z,t)$ is the axial component of the velocity field.

The quantities r_0, $t_0 \equiv (\rho r_0^3/\sigma)^{1/2}$, and ρ will be used as the characteristic length, time, and density, respectively. In addition, $\Lambda \equiv L/2r_0$ is the slenderness, $V \equiv \widetilde{V}/(\pi r_0^2 L)$ is the reduced volume, $B_0 \equiv \rho g_0 r_0^2/\sigma$ is the Bond number, and $C_\mu \equiv \mu(\rho\sigma R_0)^{-1/2}$ is the capillary number (defined as the square root of the Ohnesorge number). Finally, to measure the magnitude of the excitation, let us define the time-dependent Bond number $B(t) \equiv -\rho g(t) r_0^2/\sigma$.

3. The 1D approach

3.1. 1D models

The 1D approach has often been used to describe the dynamics of jets and liquid bridges because it allows major simplifications when interface deformations of finite amplitude are present. This is not only the case in such nonlinear phenomena as breakup [20,22], but also in the linear evolution of liquid bridges with non-cylindrical equilibrium shapes [9,11,12].

In the present work, the Lee, averaged, and Cosserat models are considered to describe both linear and nonlinear vibrations of axisymmetric liquid bridges. For the problem formulated in the previous section, these models formally reduce to the set of equations [7]

$$\left(F^2\right)_t + \left(F^2 W\right)_z = 0, \tag{1a}$$

$$F^2(W_t + W W_z) + \mathcal{I}[F,W] = -F^2 P_{cz} + 3C_\mu \left(F^2 W_z\right)_z + \mathcal{V}[F,W], \tag{1b}$$

$$F(\pm\Lambda, t) = 1 \pm H, \qquad W(\pm\Lambda, t) = 0, \tag{1c}$$

$$F(z,0) = F_0(z), \qquad W(z,0) = 0. \tag{1d}$$

In the above equations and hereafter, a subscript t or z denotes the partial derivative with respect to these variables. In Eq. (1b), $\mathcal{I}$ and $\mathcal{V}$ are functionals of F and W (and of their time and space derivatives) that depend on the model considered. In addition,

$$P_c = \frac{1}{(1+F_z^2)^{1/2}}\left(\frac{1}{F} - \frac{F_{zz}}{1+F_z^2}\right) + B_0 z + B(t) z. \tag{1e}$$

3.2. The linear regime

Consider now the influence of a small-amplitude vibration. Then the functions $S \equiv F^2$ and $Q \equiv F^2 W$ can be written as the static solution plus a small perturbation, i.e.,

$$S(z,t) = S_0(z) + s(z,t), \qquad Q(z,t) = q(z,t). \tag{2}$$

The function $S_0(z) \equiv F_0^2(z)$ is obtained from the zeroth-order (static) problem [11], while $s(z,t)$ can be eliminated from the formulation of the first-order problem by considering the continuity equation (1a) at this order, i.e., $s_t = -q_z$. The result is

$$A_0 q_{tt} + A_1 q_{ttzz} + A_2 q_t + \sum_{j=1}^{4}\left[D_j \frac{\partial^j q}{\partial z^j} + E_j \frac{\partial}{\partial t}\left(\frac{\partial^j q}{\partial z^j}\right)\right] + S_0 B_t = 0, \tag{3a}$$

$$q(\pm\Lambda, t) = 0, \quad q_z(\pm\Lambda, t) = 0, \quad q(z,0) = 0, \quad q_t(z,0) = 0, \tag{3b}$$

where A_i, D_i and E_i are functionals of the equilibrium shape $S_0(z)$ and its derivatives with respect to z. These functionals depend on the model considered, the Bond number B_0, and the capillary number C_μ. Once the function $q(z,t)$ is determined from the integration of (3a), $s(z,t)$ is calculated from the continuity equation $s_t = -q_z$.

The solution of the problem (3) for non-cylindrical liquid bridges requires the use of numerical techniques. The equilibrium contour $S_0(z)$ is obtained by solving the static problem [11], and then the functions $A_i(z)$, $D_i(z)$ and $E_i(z)$ are calculated. Eq. (3a) is integrated numerically by means of the finite-difference method. The space and

time derivatives are evaluated using a centred five-point scheme and a backward five-point scheme, respectively. The interface position $s(z,t)$ is calculated from the integration of the continuity equation using Simpson's rule.

The integration of (3) provides the temporal evolution of the interface deformation and the velocity field in both the transient and periodic regimes. However, one can focus on the periodic stage by performing an analysis in the frequency domain. In the analysis, the instant at which $B(t)$ is maximum is chosen as the new origin of time $t=0$. Thus,

$$B(t) = A\omega^2 Re\left[e^{i\omega t}\right], \quad s(z,t) = Re\left[e^{i\omega t} s(z)\right], \quad q(z,t) = Re\left[e^{i\omega t} q(z)\right]. \tag{4}$$

One now has to determine the functions $s(z)$ and $q(z)$. By considering (4) in (3), one gets

$$G_0 q + G_1 q_z + G_2 q_{zz} + G_3 q_{zzz} + G_4 q_{zzzz} - S_0 A\omega^2 = 0, \tag{5a}$$

$$q(\pm\Lambda) = 0, \qquad q_z(\pm\Lambda) = 0, \tag{5b}$$

where G_i are also functionals of the equilibrium shape $S_0(z)$ and its derivatives with respect to z. These functionals depend on the model considered, the Bond number B_0, and the capillary number C_μ. Once the value of q is known, the perturbation s is obtained from the continuity equation, i.e., $s = iq_z/\omega$. The set of Eqs. (5) constitutes a typical two-point boundary-value problem that can be solved by transforming it to an initial-value problem [11].

The transfer function

$$T(\omega,t) \equiv \frac{(F-F_0)_{\max} - (F-F_0)_{\min}}{A} \tag{6}$$

is defined as the ratio of the maximum interface deformation to the amplitude of the vibration. In (6), $(F-F_0)_{\max}$ and $(F-F_0)_{\min}$ are the maximum and minimum of the perturbation $F(z)-F_0(z)$ at the instant t, respectively. Let $\widetilde{T}(\omega)$ be the maximum of $T(\omega,t)$ over a cycle. The resonance frequencies are those values of ω for which $\widetilde{T}(\omega)$ reaches a maximum. We are especially interested in the first resonance frequency ω_r. Note that if the capillary number C_μ vanishes, there is no energy dissipation and $\widetilde{T}(\omega_r) \to \infty$ [9].

Due to the linearity of (5), the Jacobian J of the transformation $\{q_{zz}(-\Lambda),\ q_{zzz}(-\Lambda)\} \to \{q(\Lambda), q_z(\Lambda)\}$ only depends on the frequency value ω (and on the values of the parameters characterizing the liquid bridge). For $C_\mu = 0$ and $\omega = \omega_r$, $q(z) \to \infty$. Therefore, the roots of $J(\omega) = 0$ must be identified as the resonance frequencies of the inviscid liquid bridge. These roots are easily found by means of a variant of the secant-method with 6-figure accuracy, using as initial guess a solution previously calculated for a similar configuration. For $C_\mu \neq 0$, the value of ω_r is calculated with 4-figure accuracy by finding the maximum of $\widetilde{T}(\omega)$ by means of the conjugate gradient method.

3.3. The non-linear regime

Here, we shall assume that the amplitude of the liquid bridge oscillation is sufficiently large so that departures from linearity must be considered, but is smaller than the minimum amplitude leading to breakup. Under this condition, one assumes that, after a certain transient regime, nonlinear periodic oscillations can be observed. Qualitative predictions for the minimum amplitude leading to breakup were obtained in Ref. [19] from the Cosserat model for configurations close to the Plateau–Rayleigh stability limit.

In this paper, the full 1D approximation (1) is solved numerically in the periodic regime. In this case, instead of the initial conditions (1d) the periodic boundary conditions

$$F(z,0) = F(z,2\pi/\omega), \qquad W(z,0) = W(z,2\pi/\omega) \tag{7}$$

are considered. As in the linear regime, the new origin of time $t=0$ is chosen as the instant at which $B(t)$ is maximum. The Lee, averaged, and Cosserat models are integrated by means of a fully implicit finite difference scheme. The continuum integration domain $[-\Lambda \leqslant z \leqslant \Lambda, 0 \leqslant t \leqslant 2\pi/\omega]$ is replaced by a rectangular mesh with nodes (i,j), where the indices $i = 1,2,\ldots,I$ and $j = 1,2,\ldots,J$ correspond to the z and t axes, respectively. The space and time derivatives are evaluated using a centred five-point scheme on the inner nodes $i = 3,4,\ldots,I-2$. To avoid including fictitious points in the calculations, forward and backward five-point schemes along the z axis are used on the nodes $i=2$ and $i=I-1$, respectively. The boundary conditions (1c) are considered for the nodes $i=1$ and $i=I$. The periodic boundary conditions (7) are considered to evaluate the time derivatives on the nodes $j = 1,2,J-1,J$.

The result of the discretization is a system of $2 \times I \times J$ nonlinear algebraic equations for the $2 \times I \times J$ unknowns $F_{i,j}$ and $W_{i,j}$, which is solved by an iterative process. The values $F_{i,j}^{(k)}$ and $W_{i,j}^{(k)}$ corresponding to iteration k are calculated as $F_{i,j}^{(k)} = F_{i,j}^{(k-1)} + f_{i,j}^{(k)}$ and $W_{i,j}^{(k)} = W_{i,j}^{(k-1)} + w_{i,j}^{(k)}$, where $F_{i,j}^{(k-1)}$ and $W_{i,j}^{(k-1)}$ are assumed to be known. The unknowns $f_{i,j}^{(k)}$ and $w_{i,j}^{(k)}$ are calculated as small perturbations of $F_{i,j}^{(k-1)}$ and $W_{i,j}^{(k-1)}$, respectively, from the linearized system of equations. The starting values $F_{i,j}^{(0)}$ and $W_{i,j}^{(0)}$ of the iterative process correspond to one of the following cases: (i) the equilibrium, (ii) the solution obtained from (5) in the linear regime, and (iii) the nonlinear solution previously obtained for a similar configuration. The iterative process is ended when $F_{i,j}^{(k)}$ and $W_{i,j}^{(k)}$ verify the system of nonlinear equations with 6-figure accuracy. It was found that the method converges to the sought values of $F_{i,j}$ and $W_{i,j}$ after a few (less than 5) iterations. In all the cases considered, the solution was practically independent of the mesh size for $I \geqslant 40$ and $J \geqslant 30$.

It must be pointed out that the integration of (1a)–(1c), (1e), and (7) directly provides the solution for the stationary oscillations without considering the transient regime. This reduces considerably the computing time and the difficulties associated with numerical instabilities, especially for configurations close to the stability limits. Nevertheless, because no integration over time is carried out from initial conditions, the volume of the solution cannot be kept fixed. Indeed, it was found that the iterations do not strictly preserve the liquid bridge volume, which does not necessarily coincide with that corresponding to the starting values $F_{i,j}^{(0)}$. This does not affect the accuracy of the solution obtained. Corrections in the numerical method may be implemented to find the solution with the desired volume, but it would lead to a more complex and time-consuming algorithm.

Rivas and Meseguer [18] obtained a self-similar solution of the Cosserat model through a nonlinear analysis based on the singular perturbation method. The solution was derived for configurations asymptotically close to the Plateau–Rayleigh stability limit $\Lambda \to \pi$ (and, consequently, $V \to 1$, $B_0 \to 0$, and $H \to 0$) and for small frequencies. The functions S and Q are expanded in powers of a perturbative parameter ε that measures the difference between the slenderness of the liquid bridge and the value of the Plateau–Rayleigh stability limit. By considering terms up to orders $\varepsilon^{1/2}$ and ε one gets

$$S = S_0 + a \sin\left(\frac{\pi z}{\Lambda}\right) \quad \text{and} \quad Q = a_t\left[1 + \cos\left(\frac{\pi z}{\Lambda}\right)\right], \tag{8a}$$

respectively, where the amplitude $a(t)$ obeys the Duffing-type equation

$$\frac{25}{8}a_{tt} + \frac{25}{8}C_\mu a_t - \left(\frac{\Lambda}{\pi} - 1 - \frac{V-1}{2}\right)a - \frac{3}{16}a^3 + 2B = 0. \tag{8b}$$

The model (8) has recently been used to explain the behaviour of a slender liquid bridge vibrating aboard a sounding rocket [27].[2] In the present work, Eq. (8b) is numerically integrated with the initial conditions $a(0) = 2B_0/(\Lambda/\pi - 1)$ and $a_t(0) = 0$ corresponding to equilibrium. The stationary oscillations obtained after the transient regime will be compared with those calculated from both the linear and nonlinear solutions described above.

4. Results

4.1. Linear regime

Fig. 2 illustrates the transition from equilibrium to the periodic stage of a vibrating liquid bridge. The symbols represent the solution to (3) for the Cosserat model, while the solid lines correspond to the results obtained from (5) for the periodic regime. For $t \lesssim 2/|\Gamma|$ ($\Gamma = -0.1604$ is the dimensionless damping rate of the first oscillation mode [12]) a transient regime is observed, while for $t \simeq 2/|\Gamma|$ the periodic regime is practically reached. In what follows, the analysis will focus on the periodic regime.

The 1D approximation has been seen to provide good predictions for the first capillary oscillation modes of cylindrical slender liquid bridges in the limits of small and large viscosities [8] as well as for intermediate values of C_μ [10]. Good agreement with the 3D approach was also found for a vibrating axisymmetric inviscid liquid bridge [11]. In the

[2] It must be noted that, probably due to a typographical error, Eq. (6) in Ref. [27] does not coincide with that derived in Ref. [18].

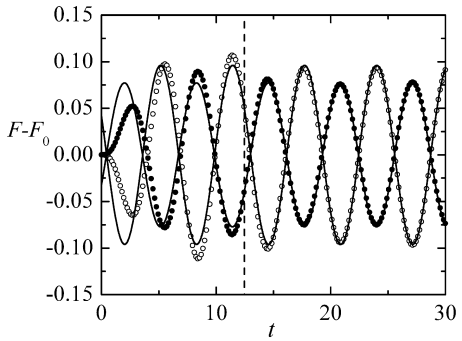

Fig. 2. Interface deformation $F - F_0$ at $z = \Lambda/2$ and $3\Lambda/2$ calculated from the Cosserat model for a vibration with $\{\Lambda = 1.6,\ V = 1.35,\ B_0 = 0.4,\ H = 0,\ C_\mu = 0.1,\ \omega = 1,\ A\omega^2 = 0.1\}$. The symbols correspond to the solution obtained from the equilibrium at $t = 0$ for $z = \Lambda/2$ (dots) and $3\Lambda/2$ (open symbols), while the solid lines are the solution in the periodic regime. The dashed line indicates the boundary $t \simeq 2/|\Gamma|$ between the transient and the periodic regimes.

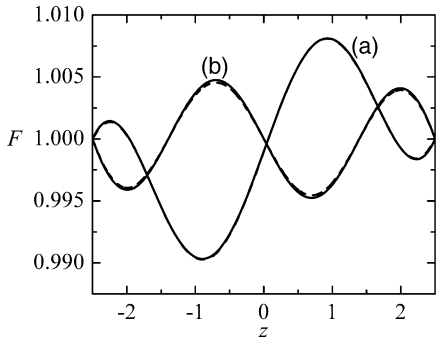

Fig. 3. Interface deformation F at $t = 0$ (a) and at $t = \pi/\omega$ (b) for $\{\Lambda = 2.5,\ V = 1,\ B_0 = H = 0,\ C_\mu = 0.1,\ \omega = 2,\ A\omega^2 = 0.05\}$. The solid and dashed lines correspond to Cosserat and 3D solutions, respectively. The lines practically overlap.

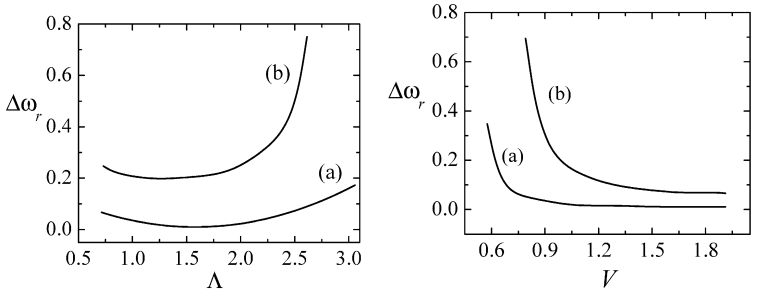

Fig. 4. $\Delta\omega_r$ obtained from the Cosserat model for $\{V = 1,\ B_0 = H = 0\}$ (left-hand graph) and $\{\Lambda = 1.6,\ B_0 = H = 0\}$ (right-hand graph), for $C_\mu = 0.1$ (a) and $C_\mu = 0.25$ (b).

present work, the 3D analysis of the free oscillations of a cylindrical viscous liquid bridge in Ref. [10] has been trivially adapted to describe the force vibrations. Fig. 3 shows the excellent agreement between the 3D and Cosserat model results for a moderately slender liquid bridge, in spite of the angular speed being much greater than the first resonance frequency $\omega_r = 0.394$. The same agreement has been observed for other configurations with similar values of Λ and ω, and intermediate values of C_μ.

The influence of the parameters characterizing the liquid bridge on its first resonance frequency ω_r was analyzed with both the 3D description and the Cosserat model in the inviscid case $C_\mu = 0$ [11]. For the sake of completeness, some results illustrating the role played by the viscosity are presented here. Fig. 4 shows the value of $\Delta\omega_r \equiv (\omega_r - \omega_r^{(0)})/\omega_r^{(0)}$, where ω_r and $\omega_r^{(0)}$ are the values calculated from the Cosserat model for $C_\mu \neq 0$ and $C_\mu = 0$, respectively. As could be expected, $\Delta\omega_r > 0$ and hence the viscosity force is a stabilizing factor which increases the resonance frequency [9]. As was previously observed for the free oscillations [12], the influence of the viscosity on the vibration is more noticeable for short liquid bridges and close to the stability limits (the Plateau–Rayleigh limit in the left-hand graph and the minimum volume stability limit in the right-hand graph). In the first case, the viscous stresses increase as the slenderness decreases, while in the second case the capillary force decreases more rapidly than the viscous force as the configuration approaches the stability limit.

4.2. Nonlinear regime

The main goal of the present paper is to analyze the nonlinear effects on the vibration of an axisymmetric liquid bridge in the periodic regime using the 1D approximation. To this end, the system of Eqs. (1a)–(1c), (1e), and (7) are integrated by means of the numerical procedure described in Subsection 3.3. To verify the validity of the method,

a comparison was made with *exact* solutions obtained in two limiting cases: (i) the nonlinear static limit ($\omega \to 0$ with arbitrary values of $A\omega^2$), and (ii) the linear regime limit ($A\omega^2 \to 0$ with arbitrary values of ω).

Fig. 5 shows the convergence of the iterative process when starting from the equilibrium solution. In the left-hand graph, $\omega = 5 \times 10^{-3}$, and thus the interface deformation at $t = 0$ obtained after the iterations practically coincides with the solution of equilibrium calculated with a Bond number $B_0 + B(0)$ (the velocity field practically vanishes). In the right-hand graph, $A\omega^2 = 0.01$, and the iterative process converges to the solution of the linear problem (5) in three iterations. Other cases varying the parameters ω and $A\omega^2$ were analyzed finding similar agreement.

Fig. 6 shows the nonlinear effects on the vibration of a liquid bridge with moderately large interface deformations with respect to equilibrium (the maximum interface deformation at $t = 0$ is about 5.3%). As can be observed, the influence of the nonlinear terms is more significant on the velocity field than on the interface deformation. It must be noted that the oscillation is stable in spite of $B_0 + B(0) = 0.3$ being notably larger than the corresponding *static* stability limit [29]. This is due to the dynamical stabilization associated with the moderately high frequency and viscosity [19]. A rough estimate of the dynamical stability limit for this configuration is $B_0 + B(0) = 1.4$ [19].

The influence of the nonlinear terms on the interface evolution can be evaluated by calculating the average deviation

$$e(t) = \frac{\int_{-\Lambda}^{\Lambda} |F(z,t) - F_{\mathrm{lin}}(z,t)|\,\mathrm{d}z}{\int_{-\Lambda}^{\Lambda} |F_{\mathrm{lin}}(z,t) - F_0(z)|\,\mathrm{d}z}, \tag{9}$$

where $F_{\mathrm{lin}}(z,t)$ is the solution to the linear problem (5). For the vibration considered in Fig. 6, $e = 13.9\%$. Fig. 7 shows the results obtained for two configurations as a function of the stimulus magnitude $A\omega^2$. The figure also shows the maximum deviation $\Delta F_{\max} \equiv \max[F_{\mathrm{lin}}(z,t) - F_0(z)]$ at the instant t of the linear solution $F_{\mathrm{lin}}(z,t)$ from the equilibrium contour $F_0(z)$. As mentioned in Subsection 3.3, the volume of the liquid bridge cannot be kept fixed through the iterations that lead to the nonlinear solution. Fig. 7 shows the volume of the solution obtained as a function of $A\omega^2$. The dependence of the average deviation e on the stimulus magnitude $A\omega^2$ is practically linear in the two configurations analyzed in both graphs, although a non-monotonous behaviour is observed in the right-hand graph for $0 \leqslant A\omega^2 \lesssim 0.05$, probably due to the influence of the volume. The magnitude of the average deviation is similar in both cases, and is larger than 10% for $A\omega^2 \gtrsim 0.1$ (or $\Delta F_{\max} \gtrsim 5\%$).

One observes in Fig. 8 how the results depend on the 1D model considered. The amplitude of the oscillation is of the same order of that observed in experiments, where nonlinear effects were analyzed [27]. The linear solution to the Cosserat model is also plotted to appreciate these nonlinear effects. As in Fig. 6, these effects are more noticeable for the velocity field than for the interface deformation. However, a significant deviation $e = 20.7\%$ between the linear and nonlinear solution is obtained. The three 1D models considered provide virtually the same result. From this and other cases analyzed in this work, one can conclude that the agreement previously observed for free oscillations in the linear regime [8,13] also holds for nonlinear vibrations.

A comparison between the numerical solution to the Cosserat model and the asymptotic solution (8) is shown in Figs. 9 and 10. Fig. 9 shows the results for a configuration with $\Lambda = 3.1$. In spite of the moderately large value $\omega = 0.2$ of the angular speed (consider that, for instance, $\omega_r = 0.183$ for a cylindrical liquid bridge with $\Lambda = 3.1$ and

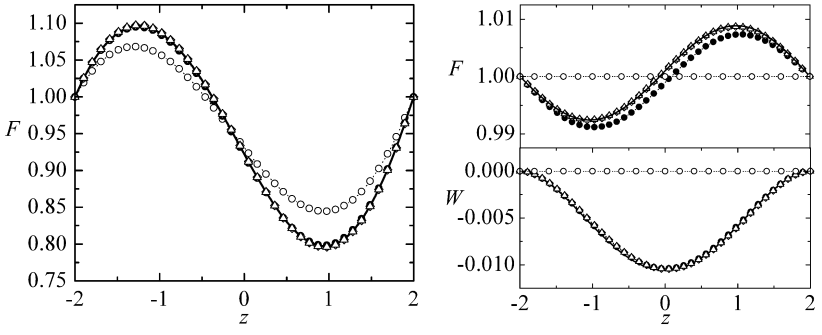

Fig. 5. The iterations $k = 0$ (○), $k = 1$ (●), $k = 2$ (◇) and $k = 3$ (△) obtained from the Cosserat model for $\{\Lambda = 2,\ V = 0.913,\ B_0 = 0.05,\ H = 0,\ C_\mu = 0.1,\ \omega = 5 \times 10^{-3},\ A\omega^2 = 0.1,\ t = 0\}$ (left-hand graph) and $\{\Lambda = 2,\ V = 1,\ B_0 = H = 0,\ C_\mu = 0.1,\ \omega = 1,\ A\omega^2 = 0.01,\ t = 0\}$ (right-hand graph). The solid lines are the nonlinear solution of the static problem for a Bond number equal to $B_0 + B(t)$ (left-hand graph), and the solution to the linear problem (5) (right-hand graph).

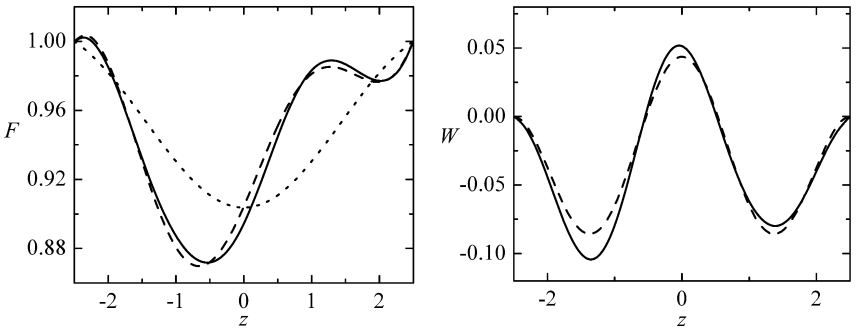

Fig. 6. Interface deformation (left-hand graph) and velocity field (right-hand graph) as obtained from the Cosserat model for $\{\Lambda = 2.5,\ V = 0.896,\ B_0 = H = 0,\ C_\mu = 0.1,\ \omega = 2,\ A\omega^2 = 0.3,\ t = 0\}$. The solid and dashed lines are the nonlinear solution and the solution to the linear problem (5), respectively. The dotted line in the left-hand graph is the equilibrium contour.

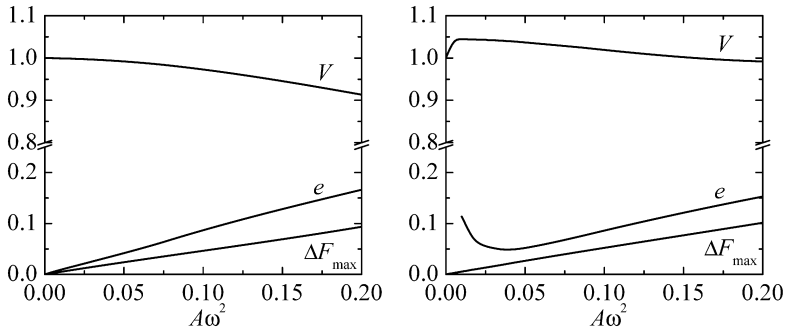

Fig. 7. Evaluation of the nonlinear effects obtained from the Cosserat model for $\{\Lambda = 2.5,\ B_0 = H = 0,\ C_\mu = 0.1,\ \omega = 1,\ t = 0\}$ (left-hand graph) and $\{\Lambda = 2.5,\ B_0 = 0.02,\ H = 0,\ C_\mu = 0.1,\ \omega = 1,\ t = 0\}$ (right-hand graph).

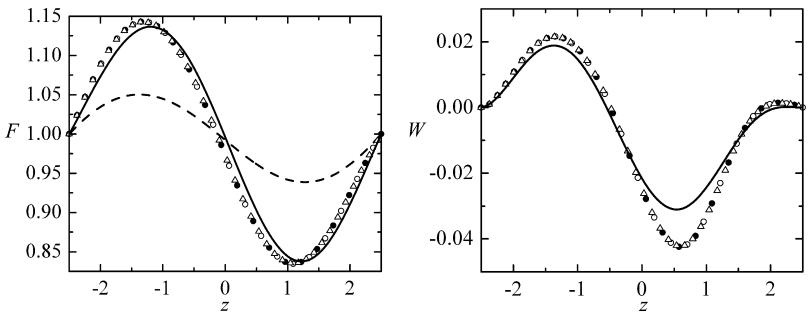

Fig. 8. Interface deformation (left-hand graph) and velocity field (right-hand graph) for $\{\Lambda = 2.5,\ V = 0.99,\ B_0 = 0.02,\ H = 0,\ C_\mu = 0.1,\ \omega = 1,\ A\omega^2 = 0.2,\ t = 2.9\}$ obtained from the Lee (△), averaged (●) and Cosserat (○) model. The solid lines are the solution to the linear problem (5) for the Cosserat model, while the dashed line corresponds to the equilibrium shape.

$C_\mu = 0.85$), the nonlinear solution (8) significantly improves the predictions of the linear approach (5). From Fig. 10 one may deduce that (8) is also accurate for configurations not asymptotically close to the Plateau–Rayleigh stability limit provided that the angular speed is small. This justifies the good agreement found in Ref. [27] between (8) and the experiments for a liquid bridge with $\Lambda = 2.83$ vibrating with a principal angular speed $\omega \simeq 0.056$. However, it is found in the present work that for, say, $\Lambda \lesssim 2.8$ and ω of the order of ω_r, (8) may be less accurate that the linear predictions (5) even for large interface deformations. In all the cases analyzed in this paper, the nonlinear corrections obtained from (8) for the interface deformation are more accurate than those calculated for the velocity field, because they are of orders $\varepsilon^{1/2}$ and ε, respectively.

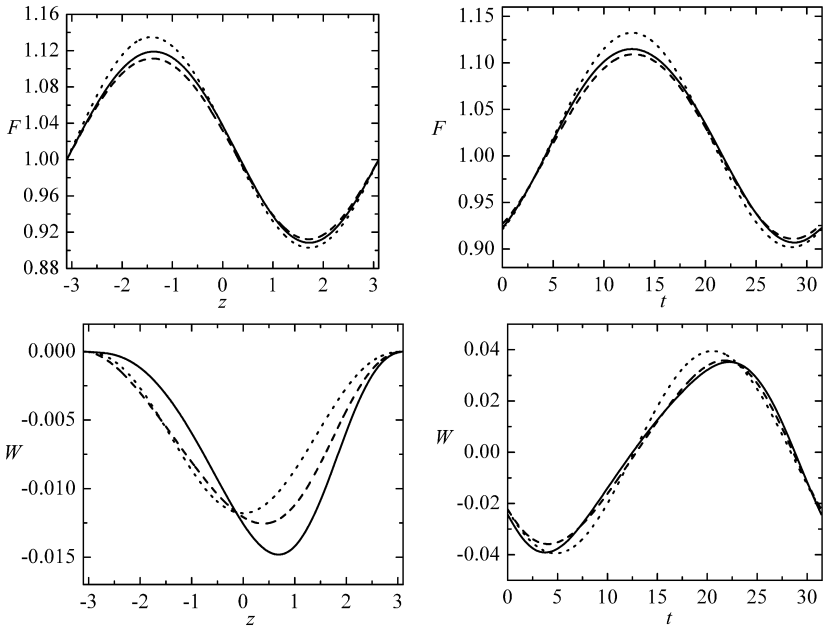

Fig. 9. Interface deformation (upper graphs) and velocity field (lower graphs) for $t = 12.8$ (left-hand graphs) and $z = -1.67$ (right-hand graphs), and for $\{\Lambda = 3.1,\ V = 1.014,\ B_0 = H = 0,\ C_\mu = 0.1,\ \omega = 0.2,\ A\omega^2 = 0.012\}$ as obtained from the nonlinear Cosserat model (solid line), the asymptotic analysis (8) (dashed line), and the solution to the linear problem (5) (dotted line).

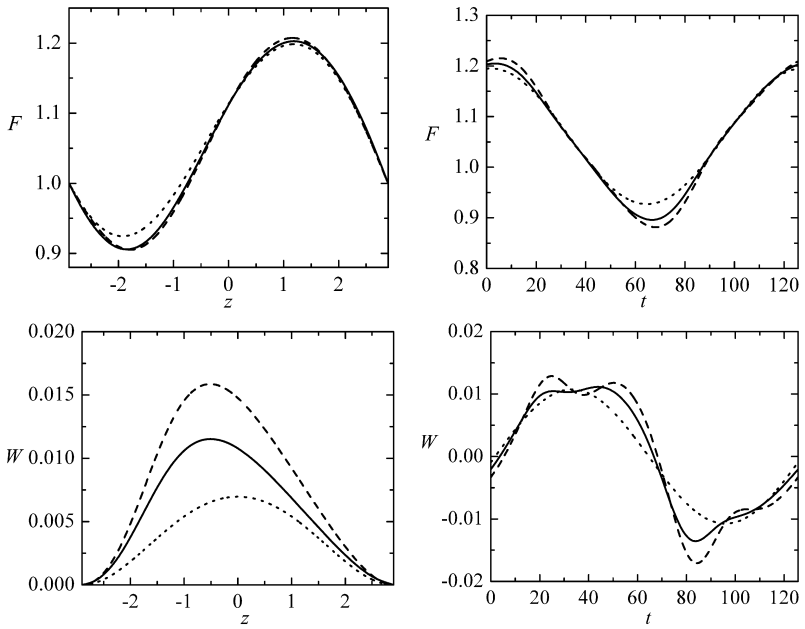

Fig. 10. Interface deformation (upper graphs) and velocity field (lower graphs) for $t = 58$ (left-hand graphs) and $z = -1.56$ (right-hand graphs), and for $\{\Lambda = 2.9,\ V = 1.13,\ B_0 = H = 0,\ C_\mu = 0.1,\ \omega = 0.05,\ A\omega^2 = 0.02\}$ as obtained from the nonlinear Cosserat model (solid line), the asymptotic analysis (8) (dashed line), and the solution to the linear problem (5) (dotted line).

5. Concluding remarks

In this paper the vibration of axisymmetric liquid bridges was analyzed numerically within the framework of the 1D approximation. Interest was mainly focused on the nonlinear effects, although some results concerning the linear

regime were also reported. Firstly, a comparison between the 3D and 1D predictions for cylindrical liquid bridges showed that the 1D approach provides very accurate results even for moderately slender liquid bridges vibrating with frequencies much larger than the first resonance frequency. It is worth mentioning that only vibrations with frequencies of the order of the first resonance frequencies are easily observed in experiments on Earth. This is because of the small value of the characteristic time t_0 associated with the microzones. Therefore, one may state that the discrepancies between the 3D and 1D approaches for, say, $\Lambda \gtrsim 2.5$ would correspond to differences smaller than the uncertainty associated with the detection of the contour in an experiment. Lastly, the influence of the viscosity on the first resonance frequency was studied by extending the results previously obtained for inviscid liquid bridges [11]. The stabilizing role played by the viscosity is clearly seen, especially for short liquid bridges and close to the stability limit.

The main findings in the nonlinear regime can be summarized as follows:

- For the cases analyzed in Figs. 6–8, the deviations between the linear and nonlinear solutions of the Cosserat model were greater than 10% for $A\omega^2 \gtrsim 0.1$ (or, equivalently, deformations from equilibrium greater than 5%). This implies that significant deviations from the linear theory would be obtained when, for instance, a microzone of water held between two disks of radius $r_0 \sim 1$ mm is subjected to accelerations greater than $0.1g_0$ (note that in this case $g_0 \sim r_0/t_0^2$).
- The results shown in Fig. 8 and other results not presented here indicate that the agreement between the Lee, average, and Cosserat models previously observed for linear oscillations [8,13] of slender liquid bridges extends to the nonlinear regime. This supports the choice of the (considerably simpler) Lee model to study complex phenomena such as the breakup process of (slender) liquid bridges [20].
- The self-similar solution derived by Rivas and Meseguer [18] yielded accurate predictions of the interface deformation even for configurations not asymptotically close to the stability limit $\Lambda = \pi$ for sufficiently small angular frequencies. For $\Lambda \lesssim 2.8$ and frequencies of the order of ω_r, nonlinear contributions are probably smaller than those neglected in the expansion (8a), and thus the linear solution (5) may improve the asymptotic solution (8).

Acknowledgement

Partial support of the Ministerio de Ciencia y Tecnología (Spain) through Grant No. ESP2003-02859 (partially financed by FEDER funds) is acknowledged.

References

[1] J.A. Nicolás, Frequency response of axisymmetric liquid bridges to an oscillatory microgravity field, Microgravity Sci. Technol. IV (3) (1991) 188–190.
[2] D. Langbein, Oscillations of finite liquid columns, Microgravity Sci. Technol. V (2) (1992) 73–85.
[3] J. Eggers, T.F. Dupont, Drop formation in a one-dimensional approximation of the Navier–Stokes equation, J. Fluid Mech. 262 (1994) 205–221.
[4] J. Meseguer, The breaking of axisymmetric slender liquid bridges, J. Fluid Mech. 130 (1983) 123–151.
[5] Y. Zhang, J.I.D. Alexander, Sensitivity of liquid bridges subject to axial residual acceleration, Phys. Fluids A 2 (1990) 1966–1974.
[6] R.M.S.M. Schulkes, Nonlinear dynamics of liquid columns: A comparative study, Phys. Fluids A 5 (1993) 2121–2130.
[7] F.J. García, A. Castellanos, One-dimensional models for slender axisymmetric viscous liquid jets, Phys. Fluids 6 (1994) 2676–2689.
[8] F.J. García, A. Castellanos, One-dimensional models for slender axisymmetric viscous liquid bridges, Phys. Fluids 8 (1996) 2837–2846.
[9] J.M. Perales, J. Meseguer, Theoretical and experimental study of the vibration of axisymmetric viscous liquid bridges, Phys. Fluids A 4 (1992) 1110–1130.
[10] J.A. Nicolás, J.M. Vega, Linear oscillations of axisymmetric viscous liquid bridges, Z. Angew. Math. Phys. 51 (2000) 701–731.
[11] J.M. Montanero, Theoretical analysis of the vibration of axisymmetric liquid bridges of arbitrary shape, Theoret. Comput. Fluid Dynamics 16 (2003) 171–186.
[12] J.M. Montanero, Linear dynamics of axisymmetric liquid bridges, Eur. J. Mech. B Fluids 22 (2003) 169–178.
[13] J.M. Montanero, F.J. Acero, A note on the use of the one-dimensional models to describe the linear dynamics of liquid bridges, Eur. J. Mech. B Fluids 24 (2005) 288–295.
[14] A. Sanz, The influence of the outer bath in the dynamics of the axisymmetric liquid bridges, J. Fluid Mech. 156 (1985) 101–140.
[15] A. Gañán, A. Barrero, Free oscillations of liquid captive drops, Microgravity Sci. Technol. III (2) (1990) 70–86.
[16] S. Ahrens, F. Falk, R. Großbach, D. Langbein, Experiments on oscillations of small liquid bridges, Microgravity Sci. Technol. VII (1) (1994) 2–5.

[17] M.P. Mahajan, M. Tsige, S. Zhang, J.I.D. Alexander, P.L. Taylor, C. Rosenblatt, Resonance behavior of liquid bridges under axial and lateral oscillating total body forces, Exp. Fluids 33 (2002) 503–507.
[18] D. Rivas, J. Meseguer, One-dimensional self-similar solution of the dynamics of axisymmetric slender liquid bridges, J. Fluid Mech. 138 (1984) 417–439.
[19] J. Meseguer, M.A. González, J.I.D. Alexander, Dynamic stability of long, axisymmetric liquid bridges, Microgravity Sci. Technol. VII (3) (1994) 246–251.
[20] J. Eggers, Nonlinear dynamics and breakup of free-surface flows, Rev. Mod. Phys. 69 (1997) 865–929.
[21] X. Zhang, R.S. Padgett, O.A. Basaran, Nonlinear deformation and breakup of stretching liquid bridges, J. Fluid Mech. 329 (1996) 207–245.
[22] A. Ramos, F.J. García, J.M. Valverde, On the breakup of slender liquid bridges: Experiments and a 1-D numerical analysis, Eur. J. Mech. B Fluids 18 (1999) 649–658.
[23] T. Chen, J. Tsamopoulos, Nonlinear dynamics of capillary liquid bridges: theory, J. Fluid Mech. 255 (1993) 373–409.
[24] D.J. Mollot, J. Tsamopoulos, T. Chen, N. Ashgriz, Nonlinear dynamics of capillary liquid bridges: experiments, J. Fluid Mech. 255 (1993) 411–435.
[25] J.A. Nicolás, J.M. Vega, Weakly nonlinear oscillations of nearly inviscid axisymmetric liquid bridges, J. Fluid Mech. 328 (1996) 95–128.
[26] J.A. Nicolás, D. Rivas, J.M. Vega, On the steady streaming flow due to high-frequency vibration in nearly inviscid liquid bridges, J. Fluid Mech. 354 (1996) 147–174.
[27] I. Martínez, J.M. Perales, J. Meseguer, Non-linear response of a liquid bridge to a sinusoidal acceleration under microgravity, Exp. Fluids 37 (2004) 775–781.
[28] I. Martínez, J. Meseguer, J.M. Perales, Wobbling of a liquid column between unequal discs, Adv. Space Res. 36 (2005) 26–35.
[29] L.A. Slobozhanin, J.M. Perales, Stability of liquid bridges between equal disks in an axial gravity field, Phys. Fluids A 5 (1993) 1305–1314.